A Field Theoretic Approach to the Analysis of Practical Coupled Dielectric Resonators

Tapan K. Sarkar and Chaowei Su
Dept. of Electrical Engineering and Computer Science
Syracuse University
http://web.syr.edu/~tksarkar

Antonije R. Djordjevic and Branko Kolundzija
Dept. of Electrical Engineering
University of Belgrade

Magdalena Salazar-Palma
Dpto de Senales, Sistemas y Radiocommunication
Polytechnique University of Madrid

Jose Luis Caceras
Alcatel Space
Madrid

ABSTRACT: Conventional methods for the analysis of dielectric resonators utilize the mode-matching technique. Other methods [1-4] have also been used. However, most of the analysis exist for analysis of single resonators. However, for practical dielectric resonators (when more than one loaded cavity is used) there may be apertures coupling one resonator to the other. In addition there may be probes coupling one resonator to the other to carry out response shaping or even cancel out the effects of the higher order modes. Also, probes may be utilized to couple energy into and out of the resonators. The high dielectric constant resonator is generally placed on top of a low dielectric constant material for support. Hence an effective analysis modeling is necessary which will predict the actual experimental data accurately if the appropriate material properties are correctly specified for coupled multiple dielectric resonators. This includes analysis of dielectric resonators with aperture couplings along with probe feeds.

FORMULATION

The objective of this paper is to describe a methodology for the analysis of multiple coupled practical dielectric resonators which will predict the experimental data within 1% accuracy. A limit of 1% is set up as our design goal as there may be various uncertainties associated with the dielectric constant and loss tangent of the various materials. The actual shapes of the probes connected to the SMA connectors that will excite the cavities is also in question. In this paper a field theoretic approach is taken for the analysis of the dielectric resonators and the results are compared with the experimental data. A 2 cavity and a 8 cavity loaded dielectric resonator structures are considered in this paper as shown in Figures 1 and 2. The resonators are coupled through an aperture as shown. In addition they are excited by probes connected to the input and output SMA connectors.

The conducting structures which include the various conducting cavities and the probes are replaced by surface equivalent electric currents. So a $\mathbf{J}_c$ is placed on the various conducting structures in free space. The original problem is sketched in Figure 3. The equivalent problem for the conductors is shown in Figure 4. All the dielectric structures are replaced by two equivalent problems, one internal and the other external. For the internal equivalent problem the internal region S_{in} as shown in Fig. 5 is bounded by two equivalent surface electric and magnetic currents as shown by $-\mathbf{J}_d$ and $-\mathbf{M}_d$. The two equivalent currents $-\mathbf{J}_d$ and $-\mathbf{M}_d$ are placed there so that they produce the correct fields in the material medium inside the structure and zero field outside. As there is zero fields produced outside, the materials of the external region can be replaced by the same equivalent material that is inside the region. The result is that the currents $-\mathbf{J}_d$ and $-\mathbf{M}_d$ produce fields that are radiating in a homogeneous region and hence it is quite straightforward to theoretically predict the fields as shown later.

For the external equivalent problem the external region where it meets the internal region has a equivalent surface currents $\mathbf{J}_d$ and $\mathbf{M}_d$. This is shown in Figure 4. So that when the internal (Fig. 5) and the external (Fig. 4) equivalent problems are superposed one on top of the other the two added surface equivalent electric and the magnetic currents add to zero and one obtains the original field problem.

For the external equivalence, we have the external sources and in addition $\mathbf{J}_d$ and $\mathbf{M}_d$ which produce the correct fields outside and zero fields inside the material. Since the currents produce zero fields inside the material the internal materials may be replaced by the same materials that exist in the external problem. Hence in this case the two currents produce the correct fields in the external region and zero fields internally and radiate in a homogeneous medium.

FIELD EQUATIONS

Next the appropriate field equations are written for the analysis.

On all conducting surfaces S_c, the total tangential electric field produced by the electric currents $\mathbf{J}_c$ and $\mathbf{J}_d$ and the magnetic current $\mathbf{M}_d$ is zero.

$$\mathbf{E}_{tan}[\mathbf{J}_c ; \mathbf{J}_d ; \mathbf{M}_d] = 0 \quad \text{for} \quad r \varepsilon S_c \tag{1}$$

Here the subscript tan referrers to the tangential components of the fields. For the external equivalent problem the total electric field produced by the currents is zero on the dielectric surfaces at a field point of $r \varepsilon S_d^-$. So that

$$\mathbf{E}_{tan}[\mathbf{J}_c ; \mathbf{J}_d ; \mathbf{M}_d] = 0 \quad \text{for} \quad r \varepsilon S_d^+ \tag{2}$$

For the internal equivalent problem, the total electric field is produced by

$$\mathbf{E}_{tan}[-\mathbf{J}_c ; -\mathbf{M}_d] = 0 \quad \text{for} \quad r \varepsilon S_d^- \tag{3}$$

Hence we have 3 equations from which the three equivalent currents can be calculated.

$$\mathbf{E}_{tan}[\mathbf{J}_c ;\mathbf{J}_d ; \mathbf{M}_d] = \mathbf{E}_{tan}[\mathbf{J}_c] + \mathbf{E}_{tan}[\mathbf{J}_d] + \mathbf{E}_{tan}[\mathbf{M}_d] \tag{4}$$

$$\mathbf{E}[\mathbf{J}] = \{k^2\mathbf{A} + \nabla\nabla \cdot \mathbf{A}\} / (j\omega 4\pi\varepsilon_o) \tag{5}$$

where

$$\mathbf{A} = \frac{\mu}{4\pi} \int_s \mathbf{J}(\bar{r}') \, G(\bar{r}|\bar{r}') \, dr' \tag{6}$$

and $S = S_c$ for $\mathbf{J} = \mathbf{J}_c$ or $S = S_d$ for $\mathbf{J} = \mathbf{J}_d$. The quantities $\bar{r}$ and $\bar{r}'$ are the field and source coordinates respectively.

$$\mathbf{E}[\mathbf{M}_d] = -\nabla \times \mathbf{F} \tag{7}$$

where

$$\mathbf{F} = \frac{1}{4\pi\varepsilon} \int_{s_d} \mathbf{M}_d(\bar{r}') \, G(\bar{r}|\bar{r}') \, d\bar{r}' \tag{8}$$

and $G(\bar{r}|\bar{r}')$ is the free space Green's function given by

$$G(\bar{r}|\bar{r}') = \frac{e^{-jk|\bar{r}-\bar{r}'|}}{|\bar{r}-\bar{r}'|} \tag{9}$$

and

$$|\bar{r}-\bar{r}'| = \{(x-x')^2 + (y-y')^2 + (z-z')^2\}^{1/2} \tag{10}$$

NUMERICAL PROCEDURE

The conducting cavities are modeled by rectangular patches of current where entire domain polynomial basis functions are applied. The use of entire domain polynomial basis over each rectangular patches not only guarantees the continuity of the current and charge over each rectangular patch but also allows for the continuity of the current across patches. Polynomial basis over each subsection is used for the current distribution on the wires. The use of entire domain polynomial basis allows for the use of much larger subsections (~2λ) than the typical 0.1λ taken usually in various method of moments applications.

The circular dielectric structures are represented by octagons of equivalent surface area. This is true not only for the dielectric resonator but also for the circular post that is used to support the high dielectric constant material.

RESULTS

As an example consider Fig. 1. One of the probe excites the first cavity and the second probe measures the strength of the signal inside the second cavity. The two cavities are coupled by an aperture. The two cavities are rectangular. The theoretical s_{21} parameters is shown in Fig. 6 along with the measured data. The experimental data is shown by the solid line and the theoretical results from this analysis is shown by the dotted lines. The differences in the between peak the theoretical and experimental data is better than 0.4%. However the theoretical data show a broader 10dB point than the experimental data.

For the second example consider a eight cavity structure, where in addition to the various cavities being connected by apertures there are probes coupling different cavities. The theoretical and the experimental data is shown in Fig. 7. The differences between the theory and experiment may be due to the various tuning screws that are there on the structure to obtain a good experimental data. Their effects are not included in theory. There is a shift of 0.5% in the response between theory and experiment. The theory in both cases represents accurately the resonance phenomenon but the levels differ because of uncertainty in the modeling of the coupling SMA connectors and the various tuning screws on the cavities and the dielectric resonators.

CONCLUSION

A dynamic field theoretic approach is presented to analyze coupled dielectric resonators. The differences between the theoretical and experimental data is better than 1% in absolute accuracy in the presence of uncertainties in material properties.

REFERENCES

[1] D. Kajfez and P. Guillon, Eds., Dielectric Resonators, Norwood, MA: Artech, 1986.

[2] R. K. Mongia, A. Ittipiboon, Theoretical and Experimental Investigations on Rectangular Dielectric Resonator Antennas, IEEE Trans. Antennas Propagat., vol. 45, no. 9, p. 1348-1356, 1997.

[3] N. Kaneda, B. Houshmand, and T. Itoh, FDTD Analysis of Dielectric Resonators with Curved Surfaces, IEEE Trans. MTT, vol. 45, no. 9, p. 1645-1649, 1987.

[4] R. K. Mongia, Theoretical and Experimental Resonant Frequencies of Rectangular Dielectric Resonator Antennas, Proc. IEE, vol. 139, pt. H, p. 98-104, Feb. 1992.

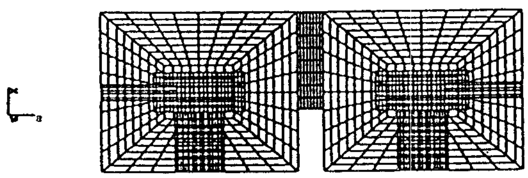

Figure 1: A two cavity coupled dielectric resonators

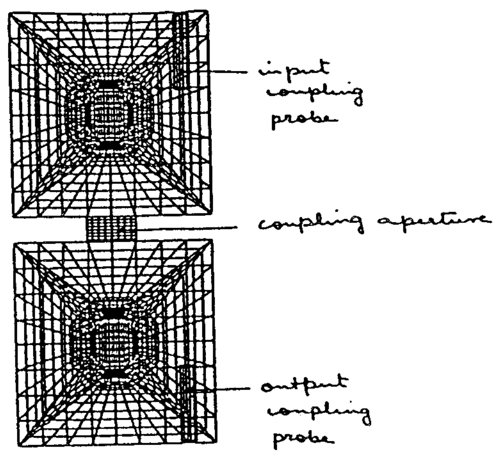

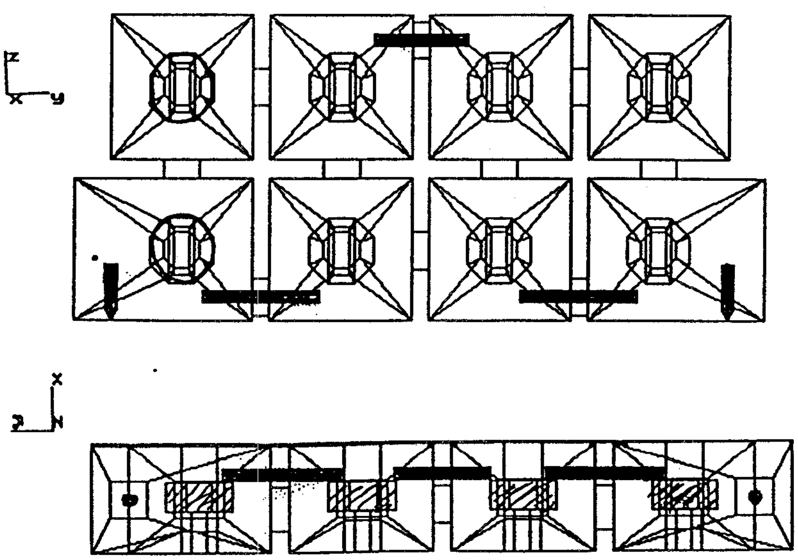

Figure 2: An eight cavity coupled dielectric resonator

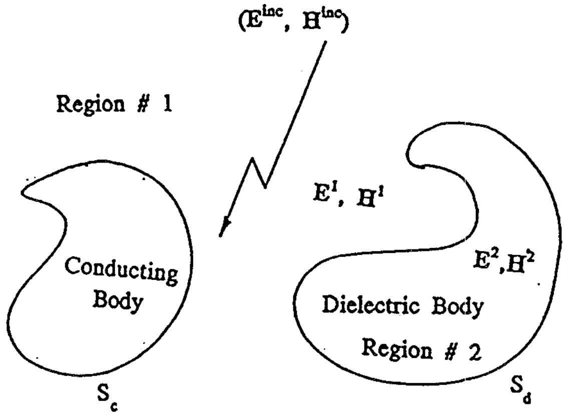

Fig 3: Original Problem.

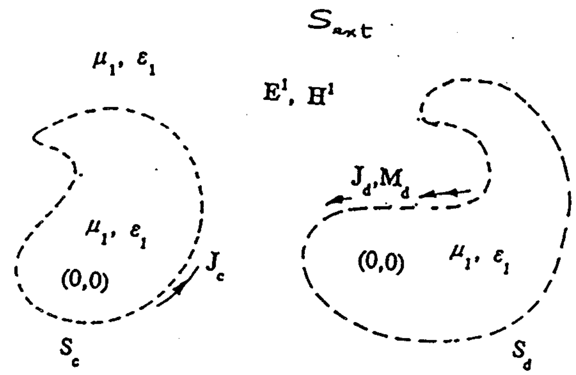

Fig 4: External Equivalence.

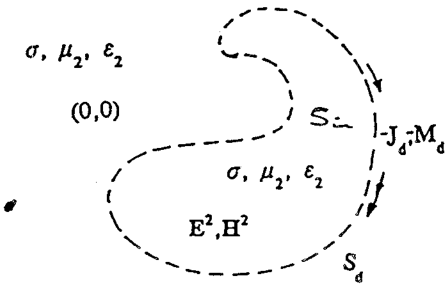

Fig 5: Internal Equivalence.

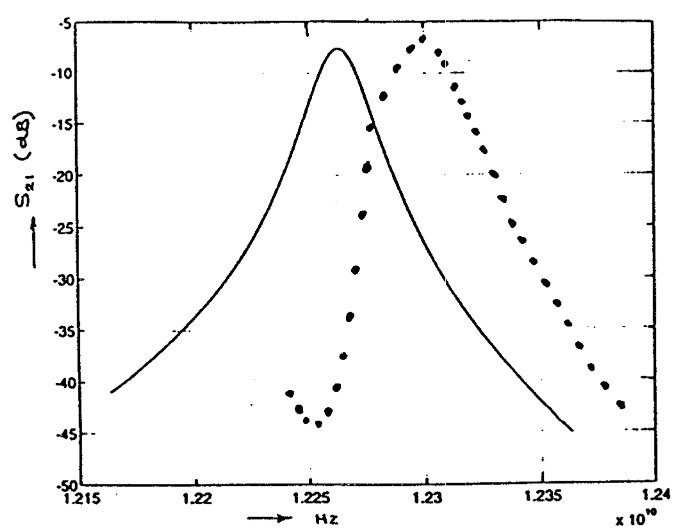

2-cavity

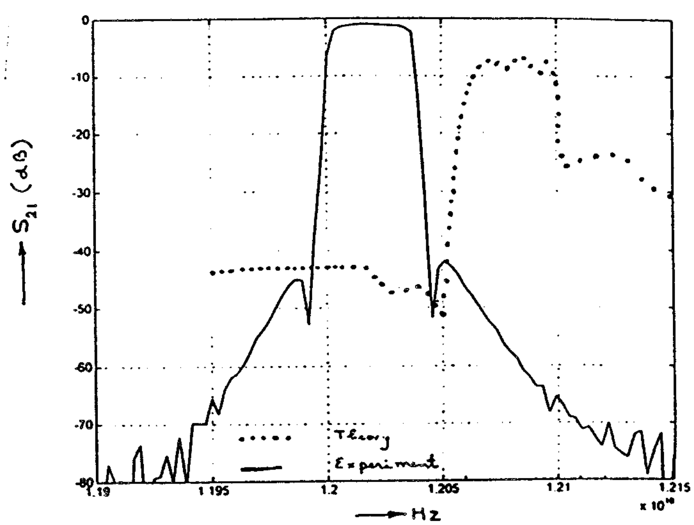

8-cavity

Figures 6 & 7: Comparison between theoretical (···) and Experimental data (——).